

## Investigation of the Dielectric Properties and Thermodynamic Parameters of $(50 - x) \text{P}_2\text{O}_5 - x\text{AgI} - 40\text{Ag}_2\text{O} - 10\text{Fe}_2\text{O}_3$ Ionic Glass

S. Abouelhassan\*

*Physics Department, Faculty of Science, Banha University, Banha, Egypt*

(Received December 24, 2008)

Fast ion conducting glasses in the form  $(50 - x)\text{P}_2\text{O}_5 - x\text{AgI} - 40\text{Ag}_2\text{O} - 10\text{Fe}_2\text{O}_3$  [where  $x = 0, 15, 20, 25, 30, 35, 40,$  and  $45$  mole %] were prepared by the melt quenching technique. The effect of frequency and temperature on the dielectric parameters, such as the dielectric constant  $\epsilon'$ , dielectric loss  $\epsilon''$ , and the dielectric loss tangent ( $\tan \delta$ ), have been studied in the temperature range 300–413 K and in the frequency range 0.5–100 kHz. The influence of adding AgI, at the expense of  $\text{P}_2\text{O}_5$ , on the dielectric properties and thermodynamic parameters of the investigated sample has been discussed in terms of suitable models. The thermodynamic parameters, such as the free energy of activation ( $\Delta F$ ), the enthalpy of activation ( $\Delta H$ ), the entropy of activation ( $\Delta S$ ), and the activation energy of relaxation ( $\Delta E_r$ ), have been calculated.

PACS numbers: 61.43.Fs, 51.30.+i, 77.22.-d

### I. INTRODUCTION

Superionic materials are a class of materials which possess ionic conduction similar to that of molten salt. This type of materials has a conductivity up to  $1 (\Omega \text{ cm})^{-1}$ , while most solids have ionic conductivities only up to  $10^{-8} (\Omega \text{ cm})^{-1}$ . The studies on the fast ionic conducting glasses are increasing due to their potential application in various electrochemical devices [1–5], such as solid state batteries, coulometer timers, fuel cells, electrochromic, and memory devices [6]. The ion conducting glasses have a number of advantages due to their isotropic nature, the absence of grain boundaries, the ease of their preparation in various bulk forms, powders, and thin films, the good possibilities for selection of appropriate components, and the possibility of varying the working characteristics over a wide range by changing their chemical composition [7–11].

Studies on silver ion conducting superionic solids in the glassy or vitreous phase have attracted widespread attention over recent years, mainly because they exhibit very high ionic conductivity at room temperature [12]. The dielectric properties of the super ionic conducting glasses have been previously studied [12–19], because more information about the conduction mechanism can be obtained. Many fast ionic conducting glasses have been synthesized in the form of binary, pseudo binary, and binary composition to obtain high ionic conductivity. The effects of adding one or more components to the ternary system, which are called quaternary fast ionic conducting glasses, have been studied [20, 21]. The aim of the present work is to investigate the effect of adding AgI, at the expense of  $\text{P}_2\text{O}_5$ , on the dielectric properties and the thermodynamic parameters of the glassy systems  $(50 - x)\text{P}_2\text{O}_5 - x\text{AgI} - 40\text{Ag}_2\text{O} - 10\text{Fe}_2\text{O}_3$  [where  $x = 0, 15, 20, 25, 30, 35, 40,$  and  $45$  mole %].

## II. EXPERIMENTAL TECHNIQUE

### II-1. Preparation of the samples

The glassy systems  $(50 - x)\text{P}_2\text{O}_5 - x\text{AgI} - 40\text{Ag}_2\text{O} - 10\text{Fe}_2\text{O}_3$  [ $x = 0, 15, 20, 25, 30, 35, 40,$  and  $45$  mole %] were prepared by melting mixtures of  $\text{NH}_4\text{H}_2\text{PO}_4$ ,  $\text{AgI}$ ,  $\text{Ag}_2\text{O}$ , and  $\text{Fe}_2\text{O}_3$  in the powder form. The mixture was heated in porcelain crucibles at temperatures ranging from  $250^\circ\text{C}$  to  $350^\circ\text{C}$  for two hours. After that, the temperature was raised gradually to  $950^\circ\text{C}$  and maintained for 6 hours in order to complete the chemical reaction. Then, the melt was shaken several times to ensure homogeneity. The melt was poured on a steel plate kept at  $0^\circ\text{C}$ . Silver paste, which shows ohmic contact with glass samples, was used for coating the desired electrode area. The sample before measurements was maintained at room temperature for about 10 hrs. The solid electrolyte glass  $20\text{P}_2\text{O}_5 - 30\text{AgI} - 40\text{Ag}_2\text{O} - 10\text{Fe}_2\text{O}_3$  was pulverized into grain with small sizes. The solid electrolyte powder was pressed under a desired pressure to form a pellet of 12 mm diameter and 1 mm thickness. The blocking electrode material  $\text{Ag}_2\text{S}$  was mixed with the electrolyte glass powder in a weight ratio of 2:3. It was pressed together with the solid electrolyte layer to form a two-layered pellet. Silver paste, which shows an ohmic behavior with the solid electrolyte layer, was used to coat the surface of the solid electrolyte layer to obtain a negative electrode.

### II-2. Measurements

The ac measurements have been carried out in the frequency range 500 Hz to 5 M Hz. The values of impedance ( $Z$ ), capacitance ( $C$ ), resistance ( $R$ ), and phase angle ( $\phi$ ) are directly read by a programmable automatic LCR meter (HIOK 3532 LCR HITESTER). The dielectric parameters  $\epsilon'$  (real part of the dielectric constant),  $\epsilon''$  (imaginary part of the dielectric constant) and  $\tan \delta$  (dielectric loss tangent), were calculated using the data of  $Z$ ,  $C$ ,  $R$ , and  $\phi$  at each frequency.

The dielectric constant  $\epsilon'$  of the sample is calculated using the following relation:

$$\epsilon' = \frac{t}{A} \cdot \frac{C}{\epsilon_0}, \quad (2.1)$$

where  $C$  is the capacitance of the sample,  $t$  is the thickness of the sample,  $A$  is the cross-sectional area of the sample, and  $\epsilon_0$  is the free space permittivity. In addition, the dielectric loss  $\epsilon''$  was calculated from the following relation:

$$\epsilon'' = \epsilon' \tan \delta, \quad (2.2)$$

where  $\tan \delta$  is the dielectric loss tangent calculated using the following formula:

$$\tan \delta = \omega RC, \quad \omega = 2\pi f. \quad (2.3)$$

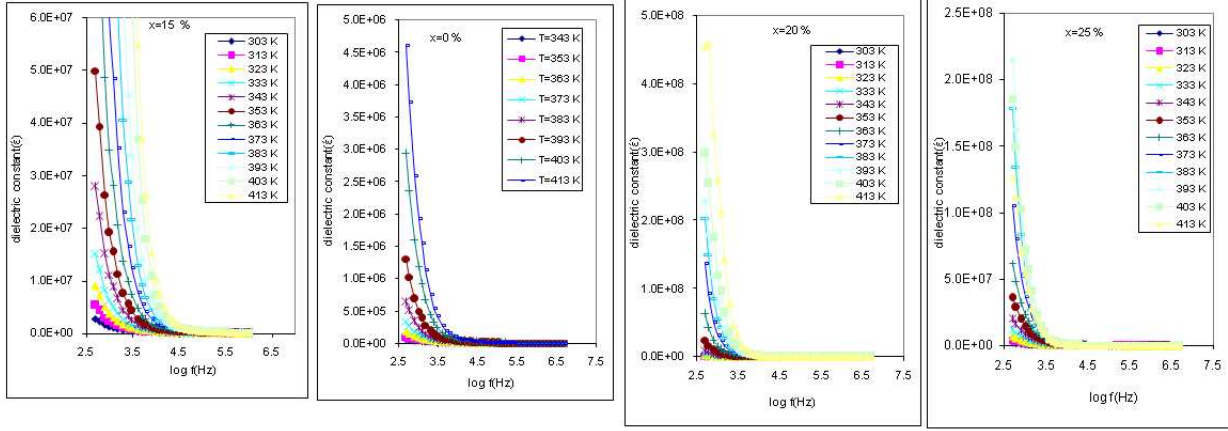


FIG. 1: The frequency dependence of the dielectric constant for the sample:  $(50 - x)\text{P}_2\text{O}_5 - x\text{AgI} - 40\text{Ag}_2\text{O} - 10\text{Fe}_2\text{O}_3$  [where  $x = 0, 15, 20, 25$ ].

### III. RESULTS AND DISCUSSION

#### III-1. Frequency and temperature dependence of the dielectric constant $\epsilon'$

Figure 1 shows the frequency and temperature dependence of the real part of the dielectric constant ( $\epsilon'$ ) for the glassy system  $(50 - x)\text{P}_2\text{O}_5 - x\text{AgI} - 40\text{Ag}_2\text{O} - 10\text{Fe}_2\text{O}_3$  [ $x = 0, 15, 20$ , and  $25$  mole %] as a representative figure, in the temperature range  $300\text{--}413$  K. The complex permittivity ( $\epsilon^*$ ) is defined by [21]

$$\epsilon^* = \epsilon' - j\epsilon'' \quad (3.1)$$

where  $\epsilon'$  is the real part of the dielectric constant and is given by  $\epsilon' = \epsilon_\infty + [(\epsilon_s - \epsilon_\infty)/(1 + \omega^2\tau^2)]$ , and  $\epsilon''$  is the imaginary part of the dielectric constant.  $\epsilon_s$  and  $\epsilon_\infty$  are the static and infinite-frequency dielectric constants. From the figure it can be noticed that, for all compositions,  $\epsilon'$  decreases with the applied frequency, and a dispersion phenomena can be observed in the low frequency range. The attenuation of the dielectric constant with frequency could be attributed to the formation of a space charge region at the electrolyte interface [5, 15, 22], which is known as the  $\omega^{n-1}$  variation or non-Debye type behavior. The behavior of the real part of the dielectric constant in the low and high frequency ranges can be explained in terms of polarizability components, as follows:

The decreasing of  $\epsilon'$  at the low frequency region may be attributed [23–27] to the contribution of a charge accumulation at the interface. For polar materials,  $\epsilon'$  depends on the contribution of multicomponents of polarizability, such as deformational (electronic and ionic) and relaxation (orientational and interfacial) polarizations. The former type of polarization depends on the electrons and ions, while the later one depends on the orientational or the interfacial effect. The high value of  $\epsilon'$  in the low frequency region may be attributed to the presence of metallic or blocking electrodes, which do not permit the mobile ions to transfer into the external circuit. As a result, the mobile ions pile

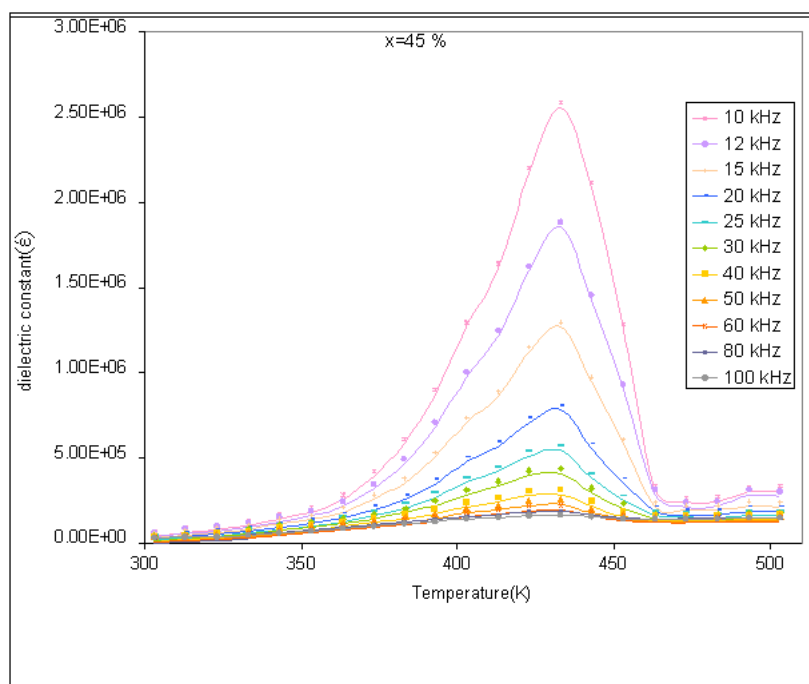


FIG. 2: The temperature dependence of the dielectric constant for the sample:  $5\text{P}_2\text{O}_5\text{-}45\text{AgI-}40\text{Ag}_2\text{O-}10\text{Fe}_2\text{O}_3$ .

up near the electrodes and give a large bulk polarization in the material. Increasing the frequency may lead to decreasing the orientational polarization, since this takes more time than electronic and ionic polarization. Such a continuous decreasing tendency of  $\epsilon'$  with increasing frequency may cause the dielectric constant to reach a constant value at higher frequency. The general behavior of  $\epsilon'$  with frequency is related to the applied field, which enhances the electron jumping between the filled and empty sites in the amorphous matrix. This will enhance the electronic components in the observed dielectric dispersion. The observed continuous decreasing in  $\epsilon'$  with frequency may be attributed to the fact that the dipoles cannot respond to the applied field.

A typical temperature dependence of the dielectric constant is shown in Fig. 2 for the sample  $5\text{P}_2\text{O}_5\text{-}45\text{AgI-}40\text{Ag}_2\text{O-}10\text{Fe}_2\text{O}_3$ . The general feature of the observed behavior is the presence of a principle peak. It has been considered [28] that the orientational polarization is related to the thermal motion of molecules, since dipoles cannot orient themselves at low temperatures. Therefore, as the temperature increases, the orientation of the dipoles becomes easier and thus increases the orientational polarization, which consequently increases the dielectric constant.

The increase of  $\epsilon'$  with temperature may be attributed [24, 29, 30, 31] at low temperatures to the small contribution of the electronic and ionic components, while the orientational component can be neglected. As the temperature increases, the ionic and electronic

polarization sources start to have a contribution to the polarizability mechanisms, which leads to the observed increase in  $\varepsilon'$ . This behavior continues up to a certain temperature (peak value of  $\varepsilon'$ ), and then a decreasing behavior of  $\varepsilon'$  with temperature can be noticed. The observed peaks for all samples were found to be in the range of the glass transition temperature of the investigated samples. From the conduction mechanism point of view, it has been considered that there exist three different ionic motions in the ionic conductive glasses which are responsible for the increase of the dielectric constant in these glasses; they are as follows:

- a. the rotation of ions around their negative sites;
- b. the short-distance transport, where the ions hop out of sites with low free energy barriers and tend to pile up at sites with high free energy barriers in the electric field direction in the dc or in a low frequency electric field, or oscillate between the sites with high free energy barriers in an ac electric field;
- c. the ions having high enough energy, which can penetrate the glasses, i.e., conduct electricity, and cause an increase in the dielectric constant. Due to the weak electrode polarization at the blocking electrode or the domain interface, one can conclude that as the temperature increases the glass network relaxes and the ionic motion becomes easier. The ions have more time to participate in the ionic conduction, causing the ionic conduction in the low frequency range to increase gradually while the dielectric properties becomes less significant; therefore the dielectric constant decreases.

### III-2. Frequency and temperature dependence of the dielectric loss $\varepsilon''$

The variation of the dielectric loss  $\varepsilon''$  with frequency for the investigated samples is shown in Fig. 3 as a representative one. It can be noticed that the dielectric loss decreases with frequency; a strong dispersion phenomena was observed at low frequencies and high temperature ranges. The observed decrease in  $\varepsilon''$  with frequency could be attributed to the formation of a space charge region at the electrode and electrolyte interface. The behavior of the space charge regions with respect to the applied frequency was explained in terms of the diffusion of ions [32].

Generally, from the observed curves in Fig. 3, the frequency dependence of  $\varepsilon''$  can be divided into two regions. The first one, which lies in the low frequency range, was attributed to the contribution of charge accumulation at the interface [23]. The second one, which lies in the high frequency range, was attributed to the high periodic reversal of the field at the interface, where the contribution of charge carriers to the dielectric loss decreases with frequency, thus  $\varepsilon''$  decreases with frequency.

The variation of  $\varepsilon''$  with temperature has been divided [33], according to the types of losses, into three parts: the conduction losses, dipole losses, and the vibrational losses. At low temperatures, the conduction losses have a minimum value, since they are proportional to  $\sigma/\omega$ . As the temperature increases,  $\sigma$  increases and consequently the conduction losses increase. This increases the value of  $\varepsilon''$  with increasing temperature.

, bb=54 187 537 743]3

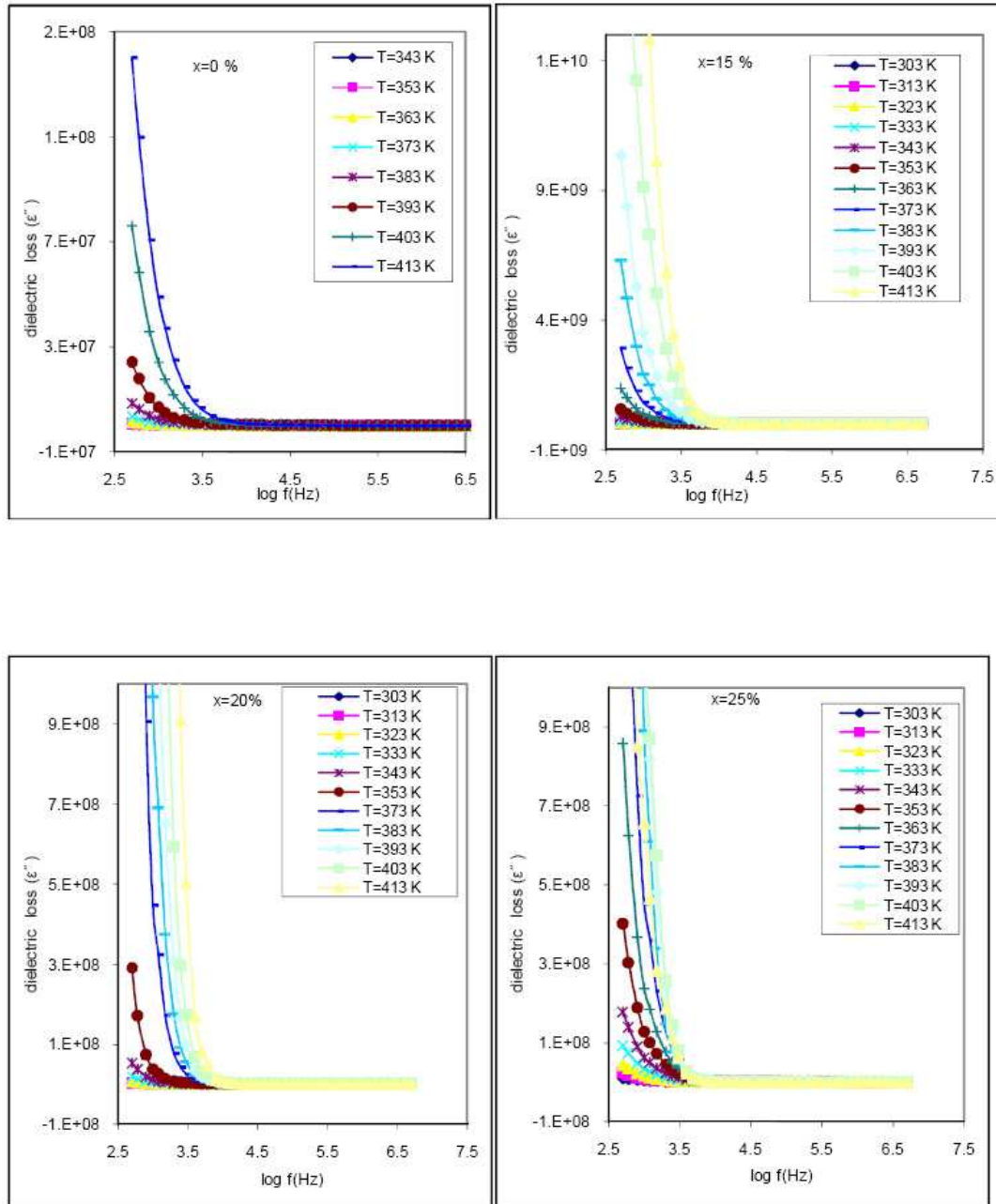


FIG. 3: The frequency dependence of the dielectric loss for the sample:  $(50-x)\text{P}_2\text{O}_5-x\text{AgI}-40\text{Ag}_2\text{O}-10\text{Fe}_2\text{O}_3$  [where  $x = 0, 15, 20, 25$ ].

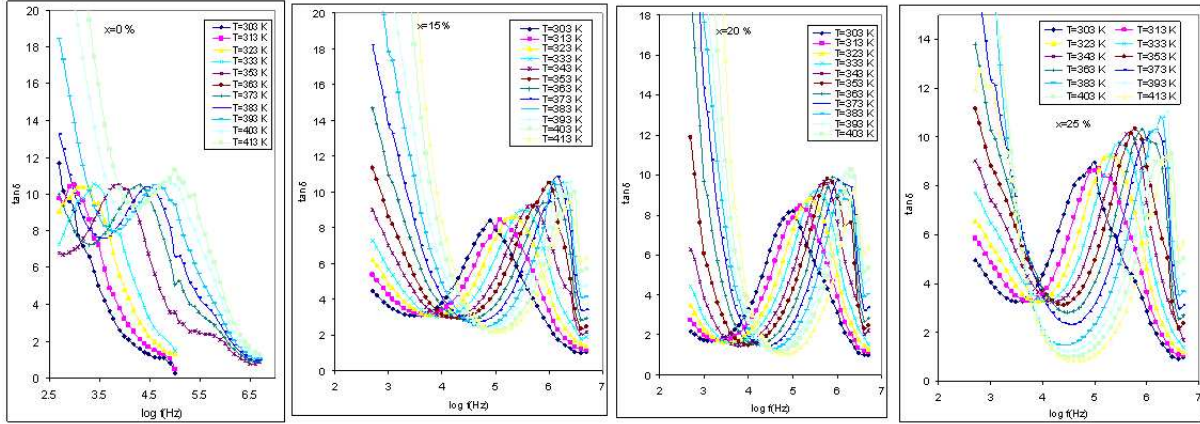


FIG. 4: The frequency dependence of the dielectric loss tangent for the sample:  $(50-x)\text{P}_2\text{O}_5-x\text{AgI}-40\text{Ag}_2\text{O}-10\text{Fe}_2\text{O}_3$  [where  $x = 0, 15, 20, 25$ ].

### III-3. Frequency and temperature dependence of the dielectric loss tangent $\tan \delta$

The effect of frequency on the dielectric loss tangent at different ambient temperatures for the samples  $(50-x)\text{P}_2\text{O}_5-x\text{AgI}-40\text{Ag}_2\text{O}-\text{Fe}_2\text{O}_3$  [where  $x = 0, 15, 20$ , and  $25$  mole %] is shown in Fig. 4 as a representative one. From the curves it can be noted that at low and moderate frequencies  $\tan \delta$  decreases dramatically, while at the high frequency range the decreasing behavior became slower, which may be attributed to the migration of ions in glasses as the main source of dielectric loss at low frequency [34].

The high values of  $\tan \delta$  at low and moderate frequencies may be attributed to the contribution of ion hopping, conduction loss, and the electron polarization loss, while the low values may be attributed to the ion vibrations. It is possible to state that, in the low frequency range, most of the Ag ions in the glassy matrix contribute to the ionic polarization. As the frequency increases the ionic polarization decreases, leading to the presence of a peak in the curves, which consequently shifts to higher frequencies with temperature. From the figure one can conclude that the peak positions shift slightly towards higher frequency, and the height of the  $\tan \delta$  peaks increases as the temperature increases. This behavior is one of the characteristics of the ionic glasses and coincides with the Debye model of dielectric relaxation.

The frequency ( $f_m$ ) corresponding to the peak value of  $\tan \delta$  is used to calculate the dielectric loss relaxation time ( $\tau$ ). When the frequency  $f$  is lower than  $f_m$ , the charge carriers are mobile over large distances and are associated with the hopping conduction. For  $f > f_m$ , the charge carriers are spatially confined to their potential wells, being mobile over short distances and associated with the relaxation polarization processes. The peak frequency  $f_m$  is an indicator of a transition from long range to short range conduction and is defined by the condition  $2\pi f\tau_m = 1$ , where  $\tau_m$  is the conductivity relaxation time. The temperature dependence of the peak frequency obeys the Arrhenius relation:

$$f_m = f_0 \exp(-\Delta E_r/KT), \quad (3.2)$$

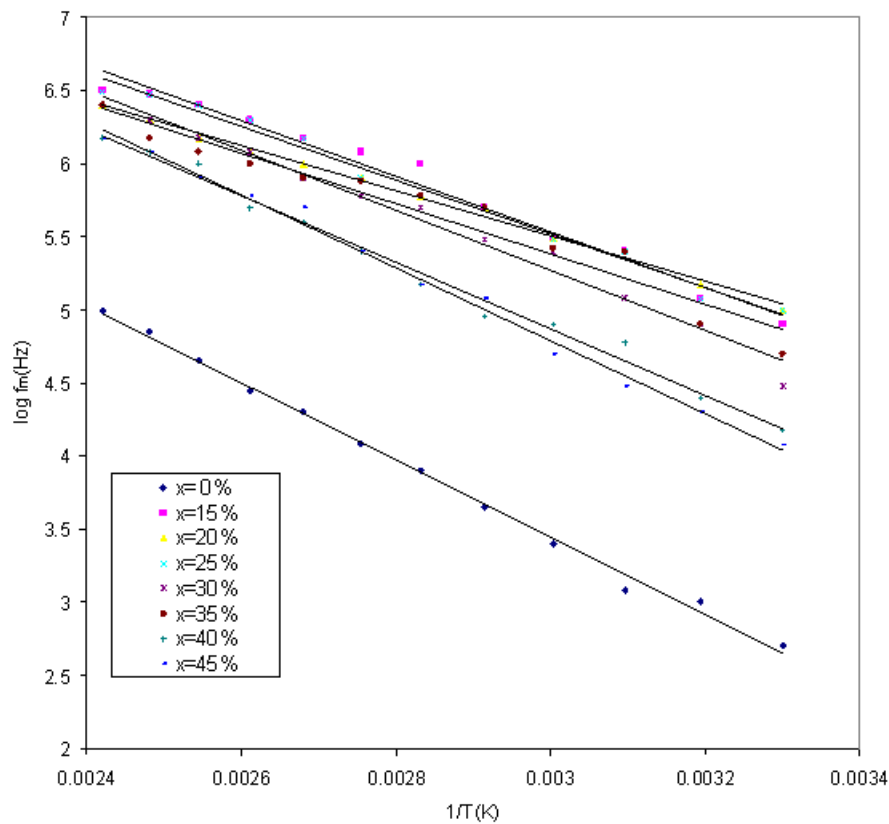


FIG. 5: The temperature dependence of the peak frequency of the dielectric loss tangent for the investigated samples.

where  $\Delta E_r$  is the activation energy of relaxation. Figure 5 shows the relation between  $\log(f_m)$  and the reciprocal temperature for different compositions. It can be noticed that a linear relation is obtained, and therefore the relaxation processes are considered to be thermally activated. The effect of AgI content on the activation energy of relaxation ( $\Delta E_r$ ) is shown in Fig. 6. The curves indicate two regions, where the first one shows a decreasing behavior down to  $x = 20\%$ , while the second one indicates an increasing behavior. The decreasing behavior in  $E_r$  may be attributed to the increase in the concentration of AgI ions in the glassy matrix, which may lead to the decrease of the relaxation time, accordingly the activation energy of relaxation decreases. Adding more AgI content leads to a structural relaxation, which in turns tends to increase the relaxation time, and therefore the activation energy of relaxation increases.



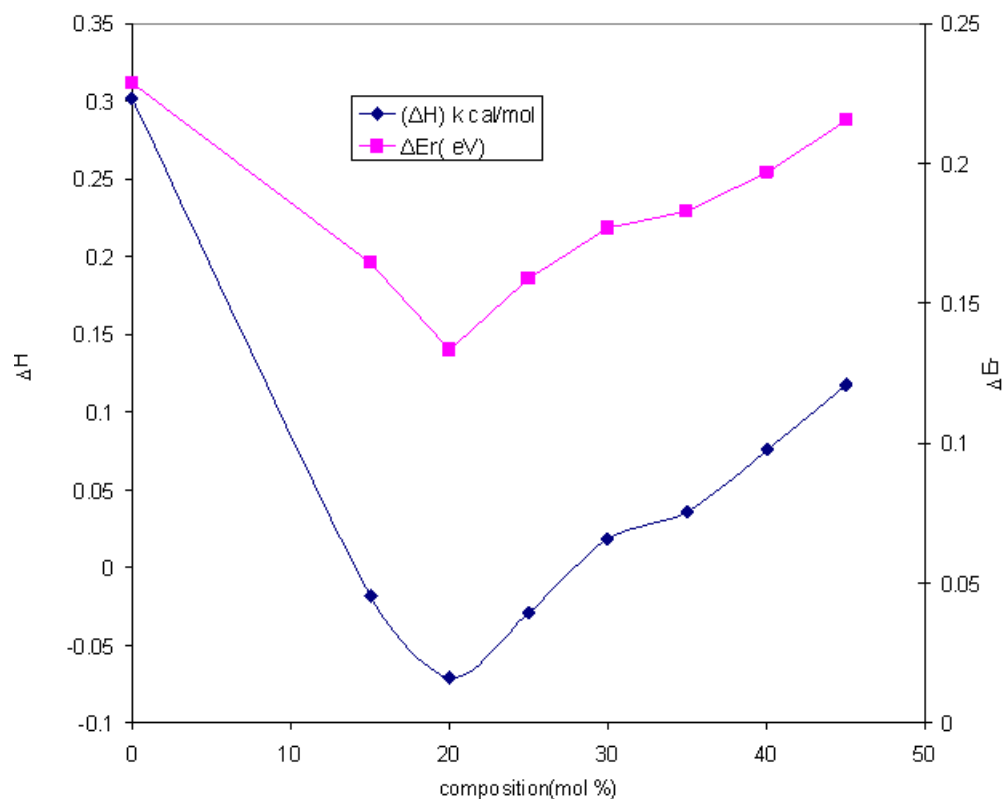


FIG. 6: The composition dependence of the enthalpy of activation and the activation energy of relaxation for the investigated samples.

#### III-4. Determination of some thermodynamic parameters

Eyring [35] was the first one who correlates the dielectric relaxation to the chemical rate theory. According to this theory the following relation was carried out [36, 37]:

$$\tau = (h/kT) \exp(\Delta F/RT), \quad (3.3)$$

where  $\Delta F$  is the free energy of activation for dipole relaxation,  $k$  is the Boltzmann constant, and  $h$  is Planck's constant. The enthalpy of activation ( $\Delta H$ ) is related to ( $\Delta F$ ) and the entropy of activation ( $\Delta S$ ) by the relation:

$$\Delta F = \Delta H - T\Delta S. \quad (3.4)$$

Equations (3.3) and (3.4) indicate that the plot of  $\log(\tau T)$  versus  $(1/T)$  should give approximately a linear relationship with a slope  $(\Delta H/R)$ , from which  $\Delta H$  can be calculated [38].

Using equation (3.4)  $\Delta F$  can be calculated by the relation

$$\Delta F = 2.303RT \log(k\tau T/h). \quad (3.5)$$

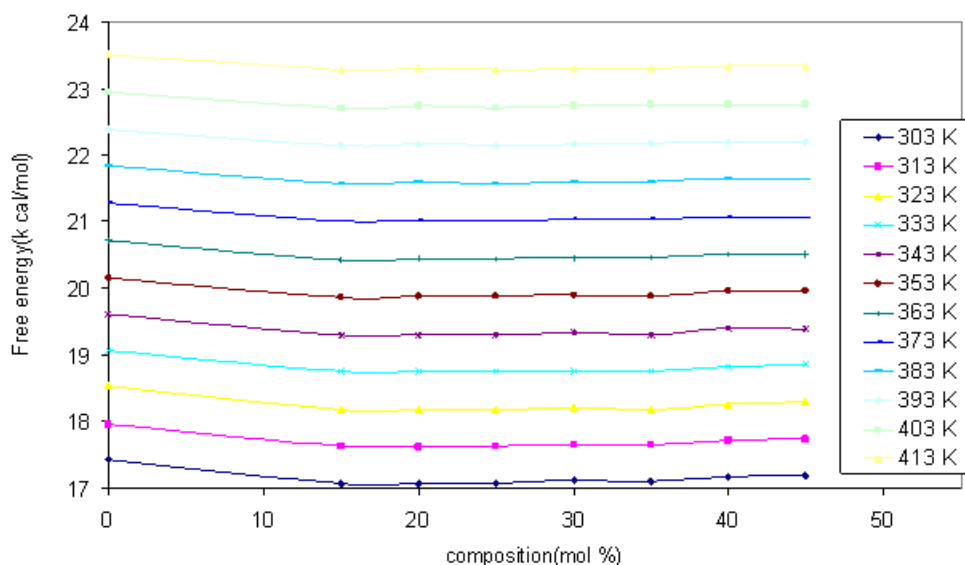


FIG. 7: The composition dependence of the free energy of activation for the investigated samples.

The relation between  $\Delta H$  and the AgI content in the sample is shown in Fig. 6. From the figure it can be noticed that  $\Delta H$  and  $\Delta E_r$  decrease gradually until the value of AgI content reaches 20%, and then a slowly increase in the curves is obtained. Figure 7 shows the effect of adding AgI on the free energy ( $\Delta F$ ) at different ambient temperatures. The decreasing behavior in  $\Delta H$ ,  $\Delta E_r$ , and  $\Delta F$  with the increase in AgI content may be explained as follows.

In the sample with  $x = 0\%$  many non-bridging oxygen bonds were found, and most of the iron ions occupy the network forming positions. Therefore the activation energy was found to be high. Increasing AgI content at the expense of  $P_2O_5$  indicates the approximate gradual decrease in the ratio of  $(P + Fe)/(O + I)$ , since Fe acts as a network former. This may lead to a decrease in the non-bridging oxygen and an increase in the Ag-p bonds, which tends to decrease the activation energy at  $x = 20\%$ . More content of AgI may increase the dangling bonds between I and P or Fe atoms of the form  $PO_3-I$  or  $FeO_3-I$ . One can expect that isolated groups of AgI may appear, leading to an increase of  $\Delta E_r$ ,  $\Delta F$ , and  $\Delta H$ .

#### IV. CONCLUSION

The dielectric properties (dielectric constant  $\epsilon'$ , dielectric loss  $\epsilon''$ , and the dielectric loss tangent  $\tan \delta$ ) of the glassy samples  $(50 - x)P_2O_5 - xAgI - 40Ag_2O - 10Fe_2O_3$  [ $x = 0, 15, 20, 25, 30, 35, 40$ , and  $45$  mole %] as a function of temperature, frequency, and

composition have been studied. The results indicated that the samples showed the dielectric phenomena such as relaxation, dispersion, and polarization, and were explained in terms of the conduction mechanisms and the Debye model. The activation energy of relaxation ( $\Delta E_r$ ) and the thermodynamic parameters [the enthalpy of activation ( $\Delta H$ ) and the free energy of activation ( $\Delta F$ )] have been deduced for the investigated samples. The effect of AgI content on these parameters showed a minimum value at  $x = 20\%$ , and the possible reason was discussed.

## References

\* Electronic address: [sayed\\_abouelhassan@hotmail.com](mailto:sayed_abouelhassan@hotmail.com)

- [1] K. P. Padmasree and D. K. Kanchan, *Material Chemistry and Physics* **9**, 551 (2005).
- [2] D. Kunze and W. Van Gool (ed.) *Fast Ionic Transport In Solids* (North Holland, Amsterdam, 1973).
- [3] B. V. R. Chowdari and S. Radhakrishnan, *Material for Solid State Batteries* (World Scientific, Singapore, 1986).
- [4] C. Suresh, *Superionic Solids: Principles and Application* (North Holland, Amsterdam, 1981).
- [5] M. Venkateswarlu, K. N. Reddy, B. Rambou, and N. Satyanarayana, *Solid State Ionics* **127**, 177 (2000).
- [6] F. A. Fusco and H. L. Tuller, *Superionic Solids and Solid Electrolytes, Recent Trends*, A. L. Lasker, and S. Chandra, eds. (New York, Academic, 1989) pp. 43.
- [7] E. Lefterova, P. Angdov, Y. Dimitriev, and Z. Stoyanov, *Analytical Laboratory* **6**, 123 (1997).
- [8] P. S. Nicholson, S. M. Whilling, G. Farrington, W. W. Smeltzer, and J. Thomast, eds., *Solid State Ionics* 91 (Amsterdam: North Holland, 1992).
- [9] T. Minami, *J. Non-Cryst. Solids* **56**, 15 (1983).
- [10] G. Chiodelli, G. C. Viganö, G. Flor, A. Magistris, and M. Villa, *Solid State Ionics* **8**, 311 (1983).
- [11] M. D. Ingram and C. A. Vincent, *Chem. Soc. Ann. Rep. A*, 23 (1977).
- [12] R. C. Agrawal and R. Kumar, *J. Phys. D: Appl. Phys.* **27**, 2431 (1994).
- [13] K. P. Padmasree and D. K. Kanchan, *J. Non-Cryst. Solids* **352**, 3841 (2006).
- [14] A. Doi, *J. Non-Cryst. Solids* **352**, 469 (2006).
- [15] F. E. Salman, N. H. Shash, H. Abouelhaded, and M. K. EL-Mansy, *J. Physics and Chem. of Solids* **63**, 1957 (2002).
- [16] F. Henn, G. Garcia-Belmonte, J. Bisquert, S. Devautour, and J. C. Giuntini, *J. Non-Cryst. Solids* **354**, 3443 (2008).
- [17] S. M. Martin, J. Schrooten, and B. Meyer, *J. Non-Cryst. Solids* **37**, 981 (2002).
- [18] M. Cutroni, A. Mandanici, P. Mustarelli, C. Tomasi, and M. Federico, *J. Non-Cryst. Solids* **307**, 963 (2002).
- [19] J. E. Garharczyk, P. Machowski, and M. Machowski, *Solids State Ionics* **157**, 269 (2003).
- [20] A. Chiodelli and A. Magistris, *Solid State Ionics* **18–19**, 356 (1986).
- [21] N. Satyanarayana, A. Karthikeyan, and M. Venkateswarlu, *J. Mater. Sci.* **31**, 5471 (1996).
- [22] M. M. Ahmed, E. Yousf, and E. Mostafa, *Physica B* **371**, 74 (2006).
- [23] F. S. Howell, R. A. Base, P. B. Macedo, and C. T. Moynahan, *J. Phys. Chem.* **78**, 639 (1974).
- [24] A. M. Farid, H. E. Atyia, and N. A. A. Hegab, *Vacuum* **80**, 284 (2005).
- [25] I. Pal, A. Agarwal, S. Sanghi, A. Sheoran, and N. Ahlawat, *J. Alloys and Compounds* **472**, 40 (2009).

- [26] T. L. Sidebottom, B. Rolling, and K. Funke, *Phys. Rev. B.* **63**, 24301 (2001).
- [27] B. Bergo, W. M. Pontusch, J. M. Prison, C. C. Motta, and J. R. Martinelli, *J. Non-Cryst. Solids* **348**, 84 (2004).
- [28] B. Tareev, *Physics of Dielectric Materials*, (Moscow: Mir Publishers, 1979), p. 107.
- [29] N. Musuhwar, M. A. M. Khan, M. Husain, and M. Zulfuquar, *Physica B* **396**, 81 (2007).
- [30] N. Mehta, D. Sharma, and A. Kumar, *Physica B* **391**, 108 (2007).
- [31] M. A. Afifi, A. E. Bekheet, E. Abdelwahhab, and H. E. Atyia, *Vacuum* **61**, 947 (2001).
- [32] J. R. Macdonald, Ed., *Impedance Spectroscopy* (Wiley, New York, 1987).
- [33] J. M. Stevels, *The Electrical Properties of Glass (Handbuch Der Physik)* 1975, pp. 350.
- [34] M. M. Elkholy and L. M. Sharaf El-Deen, *Mater. Chem. Phys.* **65**, 192 (2000).
- [35] H. Eyring, *J. Chem. Phys.* **4**, 283 (1936).
- [36] A. E. Stearn and H. Eyring, *J. Chem. Phys.* **5**, 113 (1937).
- [37] S. Glasstone, K. J. Laidler and H. Eyring, *The theory of rate process* (McGraw-Hill, New York, 1941) pp. 544.
- [38] H. A. Hashem and S. Abouelhassan, *Chinese J. Phys.* **43**, 955 (2005).